

Gamma ray spectroscopy at high energy and high time resolution at JET^{a)}

M. Tardocchi,^{1,b)} L. I. Proverbio,¹ G. Gorini,¹ G. Grosso,¹ M. Locatelli,¹ I. N. Chugonov,² D. B. Gin,² A. E. Shevelev,² A. Murari,³ V. G. Kiptily,³ B. Syme,³ A. M. Fernandes,⁴ R. C. Pereira,⁴ J. Sousa,⁴ and JET-EFDA Contributors^{5,c),d)}

¹Università degli Studi di Milano-Bicocca Istituto di Fisica del Plasma, EURATOM-ENEA-CNR Association, I-20125 Milan, Italy

²A. F. Ioffe Physico-Technical Institute, St. Petersburg 194021, Russian Federation

³EURATOM-UKAEA Association, Culham Science Centre, OX14 3DB Abingdon, United Kingdom

⁴Associação EURATOM/IST Centro de Fusão Nuclear, Instituto Superior Técnico, 1049-001 Lisboa, Portugal

⁵JET-EFDA, Culham Science Centre, OX14 3DB Abingdon, United Kingdom

(Presented 12 May 2008; received 11 May 2008; accepted 19 May 2008;
published online 31 October 2008)

In fusion plasmas gamma ray emission is caused by reactions of fast particles, such as fusion alpha particles, with impurities. Gamma ray spectroscopy at JET has provided valuable diagnostic information on fast fuel as well as fusion product ions. Improvements of these measurements are needed to fully exploit the flux increase provided by future high power experiments at JET and ITER. Limiting aspects are, for instance, the count rate capability due to a high neutron/gamma background combined with slow detector response and a modest energy resolution due to the low light yield of the scintillators. This paper describes the solutions developed for achieving higher energy resolution, signal to background, and time resolution. The detector design is described based on the new BrLa₃ scintillator crystal. The paper will focus on hardware development, including a photomultiplier tube capable of stable operation at counting rate as high as 1 MHz, the magnetic shielding, and the fast digital data acquisition system. © 2008 American Institute of Physics. [DOI: 10.1063/1.2964205]

I. INTRODUCTION

Gamma ray spectroscopy (GRS) of fusion plasmas is one of the techniques which can be used to measure and study fast particles in tokamaks.¹ Gamma ray emission is caused by reactions of fast particles with fuel ions or more frequently with impurities. In a thermonuclear plasma there are essentially three main sources of fast ions: (i) fusion product ions, as, for instance, ⁴He in DT plasma or *p*, *t*, and ³He in DD, with kinetic energies in the MeV range; (ii) acceleration of ions via ion cyclotron resonance heating (ICRH) which can give rise to suprathermal ion component with energies up to several MeV; and (iii) injection of neutral beam ions (NBI) ions with energies usually of the order of 50–150 keV. At JET, where the main plasma impurities are carbon and beryllium, gamma ray diagnostics has provided valuable diagnostic information on fast ion effects during ICRH and NBI heating, especially during the trace tritium experiment campaign.² The gamma ray spectrum depends on the specific nuclear reaction, on the energy of the interacting

particles, and on the nuclear levels of the formed nucleus which is left on an excited state. GRS is thus needed to distinguish the gamma rays and to identify the underlying reactions, which in turn allows identifying the associated fast ions giving rise to the specific gamma ray emission. In certain cases, due to the threshold or resonant nature of the nuclear cross section, it is also possible to infer the fast ion energy distribution from the relative intensities of the gamma ray peaks located at different energies.³

At JET, the gamma diagnostic system consists of a horizontal and a vertical neutron/γ camera for measurement of the emission profile from the plasma, and three collimated gamma ray spectrometers.³ Although the profile monitor camera was designed for neutron measurements it has been used in some ICRH JET discharges to measure the spatial distribution of the γ emission.⁴ Gamma ray energy spectra are measured with a BGO (3 × 3 in.²) scintillator detector with a horizontal view of the plasma. This detector, which is heavily shielded from the neutron radiation, covers gamma energies up to 28 MeV and has an energy resolution [full width at half maximum (FWHM)] of about 6% at 4 MeV. A second spectrometer is NaI(Tl) scintillator (5 × 5 in.²) detector which views the plasma vertically through the center. The NaI detector covers the energy range 1–15 MeV with a FWHM of about 3% at 4 MeV. The main limitations of these spectrometers are the high background induced by neutrons in the surrounding, a slow detector response which limits the maximum tolerable counting rate, and a modest energy resolution if compared to other type of gamma detector as, for

^{a)}Contributed paper, published as part of the Proceedings of the 17th Topical Conference on High-Temperature Plasma Diagnostics, Albuquerque, New Mexico, May 2008.

^{b)}Author to whom correspondence should be addressed. Tel.: +39 02 62482326. FAX: +39 02 66173239. Electronic mail: marco.tardocchi@mib.infn.it.

^{c)}For a full listing of names and affiliations of the JET-EFDA Contributors, see A. T. Macrander, Rev. Sci. Instrum. 79, 10F701 (2008).

^{d)}See the Appendix of M.L. Watkins *et al.*, Fusion Energy 2006 (Proceedings of the 21st International Conference, Chengdu, 2006) IAEA, (2006).

TABLE I. Comparison of properties of some inorganic scintillators used for gamma spectroscopy. LaBr_3 has been selected as the best candidate for application to GRS of thermonuclear plasmas.

	NaI	LaBr_3	BGO	LYSO
Density (g/cm^3)	3.67	5.29	7.13	7.1
Scintillation time (ns)	230	16	300	41
Refractive index	1.85	1.9	2.15	1.81
Light yield (photons/keV)	38	63	8.2	32

instance, germanium semiconductors. Improvements of the present detectors are needed to fully exploit the flux increase provided by future high power experiments at JET and ITER. In particular, ITER-related developments should include testing of new scintillator materials based on high-Z scintillators recently developed;⁵ these materials feature fast scintillation times and good light yields (see Table I), which is promising for the development of high rate measurements with reduced neutron sensitivity. Whenever possible, scintillators with low oxygen content should be used due to the unfavorable interaction of fast neutrons with oxygen leading to high background.¹

This paper describes the enhancement of the existing gamma ray spectrometers at JET within the JET-EP2 program. The project, called GRS, aims to improve the existing detectors in the key areas of energy resolution, time resolution, and signal to background. Focus of this paper will be given to the solution adopted to achieve the desired improvements. In particular, the paper will describe the hardware development, such as the detector design, a photomultiplier tube optimized for high rate operations, and the fast digital data acquisition system.

II. DEVELOPMENT OF NEW DETECTORS FOR GAMMA RAY SPECTROSCOPY

The GRS project goals are to enhance the time and energy resolutions of the today's spectroscopic measurements at JET. For the time resolution, the key figure of merit is the count rate capability which could reach 1 MHz in stable working conditions. Higher count rates (up to 5 MHz) will be achievable by tolerating pile-up effects and gain drifts which affect the detector response. These effects are unavoidable but can be quantitatively controlled and corrected for through the combined use of a control and monitoring (C&M) system and a digital data acquisition. The improvement concerning the energy resolution will be achieved with the use of a new scintillator material which features higher light yield emission than the existing scintillators.

A. Detector design

Among new inorganic scintillator materials which have recently become available for GRS $\text{LaBr}_3(\text{Ce})$ (Ref. 6) and $\text{LYSO}(\text{Ce})$ are the most promising ones for fusion applications. Their main characteristics, shown in Table I compared to those of BGO and NaI, are high density together with short scintillation times and high light yield. The best candidate for application to fusion is LaBr_3 which has the advantage over LYSO of a primary scintillation as short as 16 ns

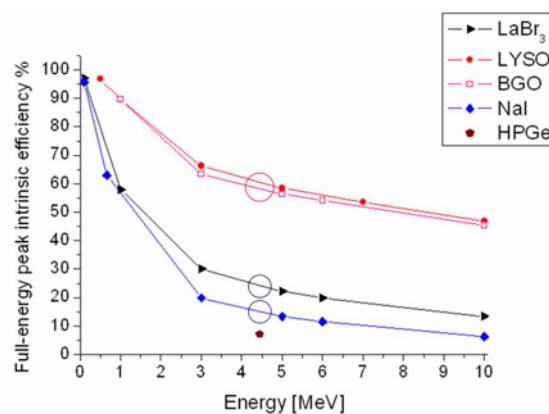


FIG. 1. (Color online) Simulation of the full energy peak intrinsic efficiency as a function of collimated monoenergetic gamma rays for detectors based on the scintillators shown in Table I. The crystal sizes are $\text{NaI}-5 \times 5 \text{ in.}^2$, $\text{BGO}-3 \times 3 \text{ in.}^2$, $\text{LYSO}-3 \times 4 \text{ in.}^2$, and $\text{BrLa}-3 \times 3 \text{ in.}^2$. For comparison it is shown also a HPGe semiconductor detector with 100% relative efficiency.

and a better light yield of 63 photons/keV. LYSO would offer higher density (and thus detection efficiency) but has the drawback of containing the radioactive isotope ^{176}Lu (2.6% isotopic abundance) which, for a large crystal, would produce a significant amount of intrinsic background (mainly β^-) radiation. Moreover, the presence of oxygen is a drawback in view of potential applications on ITER. Finally, LaBr_3 has a lower sensitivity to neutrons.

Two identical scintillator detectors based on LaBr_3 have been designed. The detector design has been made on the assumption of a crystal size $3 \times 3 \text{ in.}^2$ directly coupled to a 3 in. photomultiplier tube (PM tube). The detector performance has been simulated with photon transport calculation done with the code GEANT4 and compared to the performance of the detectors in use at JET. These simulations have determined the detection efficiency to an incoming monoenergetic gamma radiation, collimated with a 25 mm diameter. Example of results is shown in Fig. 1 where the full energy peak intrinsic efficiency, defined as the fraction of incident gammas resulting in events depositing the full energy, is shown as a function of the incoming gamma energy.⁷ We can notice that the LaBr_3 ($3 \times 3 \text{ in.}^2$) crystal features higher efficiency than the NaI detector in use at JET and reaches about 28% at 4 MeV. For comparison it is also shown that a LYSO ($3 \times 4 \text{ in.}^2$) would feature the best efficiency. Simulations of events resulting in full energy deposition relative to the total detected events (so called peak to total ratio) have shown that LaBr_3 detector is significantly better above 1 MeV than the NaI; for instance, at 4 MeV LaBr_3 reaches a peak to total ratio of about 35%, which is 50% higher than the value reached by NaI.⁷ This is important since most of the information is in the full energy peak of the detected gamma. A larger size LaBr_3 crystal (such as $3 \times 6 \text{ in.}^2$), which has become available very recently, would provide a further improvement. Concerning the improvement in energy resolution, two independent estimates based on the number of photoelectrons collected at the first dynode and on extrapolation from calibration measurements at 662 keV, respectively, yield an expected FWHM $< 2\%$ at 4 MeV.⁸ Such improvement will allow for better discrimination of gamma

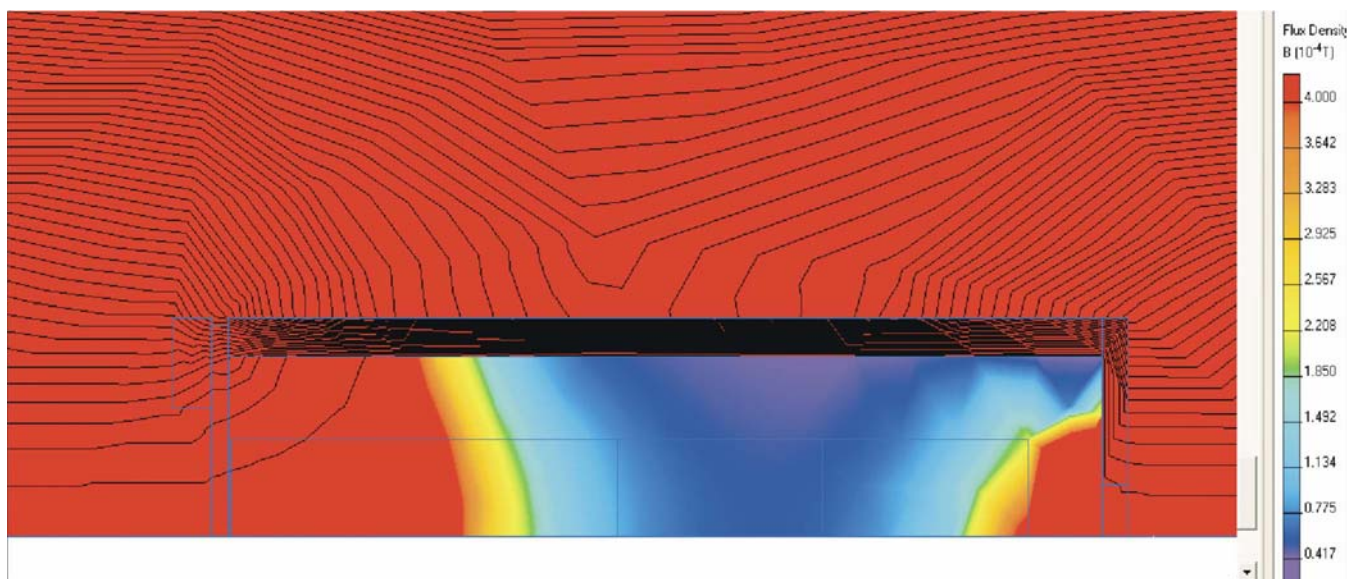


FIG. 2. (Color online) Example of simulation results of the magnetic shielding. The picture shows the modification of the magnetic field lines together with a contour plot of the magnetic field intensity for a constant field of 50 G parallel to the shielding axis. The red color represents magnetic flux densities ≥ 4 G.

lines and also analysis of the Doppler broadened shape, so far never attempted on a fusion plasma.

An important task in the project is to guarantee good detector stability. In fact, peak shifts during a JET discharge of the same level of the energy resolution, as a consequence, for instance, of gain variation of the PM tube, would distort the pulse height spectrum with an unwanted degradation of the effective energy resolution of the detector. Long term (days) stability is less critical since it implies simply a recalibration of the measured pulse height spectra, which can be easily done with the use of radioactive sources in combination with the C&M system. A short-term stability on the time scale of a JET pulse (about 120 s) better than 1% is the target value. Several factors contribute to variation of the gain of the PM tube, one of which is the sensitivity to the presence of external magnetic fields.

The detector will operate behind a collimated n/γ beam, in the roof laboratory at a distance about 23 m from the center of the tokamak. The stray magnetic field in the roof laboratory varies during a discharge; a value of 50 G has been taken as an upper limit for the intensity of the stray magnetic field at the detector location with a direction tangential to the PM-tube axis. PM tubes are well known to be very sensitive to the presence of magnetic fields. Even small fields of order of 1 G or less can affect the electron trajectories with a consequent change in collection efficiencies between the dynodes and thus in the overall gain. The size of the effect depends on the specific geometry of the PM tube and on the relative direction of the magnetic field. The most critical area is between the cathode, where the photoelectrons are produced, and the first dynode, since here the electrons travel the longest trajectories. To protect the detector a magnetic shielding has been designed with the help of software simulations. The effectiveness of the shielding to reduce the magnetic field has been studied with the finite element code QUICKFIELD.⁹ The optimized shielding is made of a soft iron cylinder of 15 mm thickness and 140 mm internal diameter

enclosing the entire detector. Additional elements made of magnetic steel have been inserted, namely, a 10 mm thick plug in the back and a 15 mm thick front ring (with a 100 mm hole for letting through the collimated γ rays without intercepting the neutron beam) which has the dual function of shielding and support structure. With such a shielding a magnetic attenuation >50 has been achieved, with values of $B \approx 0.9$ G at the PM-tube cathode. An example of the simulation result is shown in Fig. 2. Here we can note that the function of the back plate and front ring is to extend further the central region of reduced magnetic field. A dual layer of μ -metal will further reduce the magnetic field down to $B \approx 10$ mG, which is considered acceptable for PM-tube operations.

B. Photomultiplier tube for high rate operation

An important hardware component of the detector is the PM tube which collects the photons emitted from the scintillator and produces an analog signal to be recorded by the data acquisition. PM tubes are known to show variation of the gain when the counting rate of the source is varied. This is due to the fact that the mean photoelectric current running between the dynodes tends to decrease the divider chain current, and this results in a voltage drop between the last dynode and the anode which in turn cause a redistribution of all interdynode voltages and a consequent modification of the gain. A PM tube with a custom developed active base, which includes transistors in the last three stages, has been developed optimized for this application. The PM tube is an eight stage Hamamatsu R6233-01 with a length of 223 mm and a diameter of 82 mm the gain at the nominal high voltage of 1000 V is 2.7×10^5 .

The performance of the PM tube has been measured with the C&M system. The C&M system is based on two independent light emitting diodes (LED) which send light pulses via optical fibers to the PM-tube photocathode. The

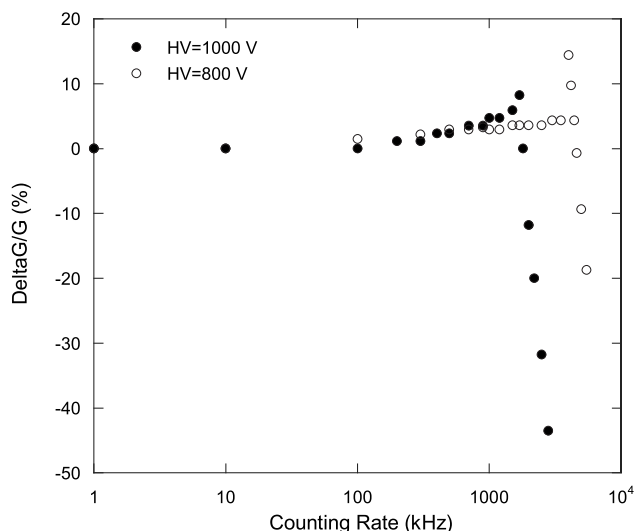


FIG. 3. Measurement of the PM tube gain variation as a function of counting rate at two different high voltage values.

LED pulse duration and intensity can be adjusted to simulate a LaBr₃ pulse. One LED is used as perturbation and is fired at a variable frequency while the second is kept at a fixed frequency (1 kHz) to monitor the PM tube gain. Using two LEDs allows having a monitoring signal which is independent of possible variations of the LED light intensity with the repetition frequency. Measurements of the gain of the PM tube as a function of the repetition rate (see Fig. 3) show that the PM tube can be operated up to a repetition frequency of 0.5 MHz with gain variations below <2%. Further increase in frequencies up to 3 MHz can be reached by tolerating a gain drop down to 50%. The operating range can be further extended up to 5 MHz by reducing the high voltage to 800 V and compensating the reduction in pulse amplitude with a fast preamplifier. Gain variations as well as pile-up events which will occur for operations at high counting rates can be corrected with the help of the C&M system and a suitable correction algorithm.

C. Digital data acquisition

Data will be acquired with a digital system which is based on the Advanced Telecommunications Computing Architecture and contains an ix86-based processor blade and a data transfer based on PCI Express links.¹⁰ Each module has eight high-speed transient recorders with 13 bit resolution and up to 400 Msamples/s sampling rate with the possibility to achieve 800 Msamples/s by interleaving two channels to-

gether. The core of the module is two field programmable gate arrays chips able to perform real-time processing algorithms such as pulse height analysis. Real time analysis of the analog pulse shapes (time and amplitude) allows a significant data reduction. Reconstruction of the pile-up events can be done off-line by storing the entire waveform whenever pile-up events occur and applying suitable algorithms.¹¹ The possibility of running these algorithms in real time on the FPGA is being investigated.

III. CONCLUSIONS

The GRS enhancement project provides an upgrade of the existing gamma spectrometers at JET. Two new scintillator detectors will be installed at JET by the end of 2008. New solutions have been developed for achieving the desired improvements in energy, time resolution, and signal to background.

ACKNOWLEDGMENTS

This work, supported by the European Communities under the contracts of Associations between EURATOM and ENEA-CNR, IST, UKAEA, was carried out within the framework of the European Fusion Development Agreement. The views and opinions expressed herein do not necessarily reflect those of the European Commission.

- ¹V. G. Kiptily, F. E. Cecil, and S. S. Medley, *Plasma Phys. Controlled Fusion* **48**, R59 (2006).
- ²V. G. Kiptily, Yu. F. Baranov, R. Barnsley, L. Bertalot, N. C. Hawkes, A. Murari, S. Popovichev, S. E. Sharapov, D. Stork, and V. Yavorskij, *Phys. Rev. Lett.* **93**, 115001 (2004).
- ³V. G. Kiptily, F. E. Cecil, O. N. Jarvis, M. J. Mantsinen, S. E. Sharapov, L. Bertalot, S. Conroy, L. C. Ingesson, T. Johnson, K. D. Lawson *et al.*, *Nucl. Fusion* **42**, 999 (2002).
- ⁴V. G. Kiptily, F. E. Cecil, S. S. Medley *et al.*, *Nucl. Fusion* **45**, L21 (2005).
- ⁵M. Moszynski, D. Wolski, T. Ludziejewski, M. Kapusta, A. Lempicki, C. Brecher, D. Winiewski, and A. J. Wojtowicz, *Nucl. Instrum. Methods Phys. Res. A* **385**, 123 (1997).
- ⁶E. V. D. van Loef, P. Dorenbos, C. W. E. van Eijk, K. W. Kraemer, and H. U. Guedel, *Appl. Phys. Lett.* **79**, 1573 (2001).
- ⁷E. C. Dell'orto, "Sviluppo di nuovi rivelatori per la spettroscopia di raggi gamma in plasmii termonucleari," Laurea degree thesis, Università degli Studi di Milano-Bicocca, 2007.
- ⁸M. Locatelli, "Nuovo sistema di spettroscopia γ per plasmii termonucleari," Laurea degree thesis, Università degli Studi di Milano-Bicocca, 2008.
- ⁹QUICKFIELD, Version 5.5, Tera Analysis Ltd.
- ¹⁰R. C. Pereira, J. Sousa, A. M. Fernandes, F. Patrício, B. Carvalho, A. Neto, C. A. F. Varandas, G. Gorini, M. Tardocchi, D. Gin, and A. Shevelev, *Fusion Eng. Des.* **83**, 341 (2008).
- ¹¹D. B. Gin, I. N. Chugunov, and A. E. Shevelev, *Instrum. Exp. Tech.* **51**, 240 (2008).